THE ASTROPHYSICAL JOURNAL, 437:63–66, 1994 December 10

LENSING FROM THE LIGHT-TRACES-MASS MAP OF MS 1224+20

R. G. CARLBERG,[1,2,3] H. K. C. YEE,[1,2] AND E. ELLINGSON[1,4]

Received 1994 February 18; accepted 1994 May 18

ABSTRACT

To compare the gravitational lensing mass with the virial mass of the MS 1224+20 cluster of galaxies, we have completed a uniform, high-precision redshift survey over a field of $7' \times 9'$, obtaining 75 redshifts. The velocity dispersion of 30 cluster galaxies is 770 km s^{-1}, and the projected harmonic radius is 0.32 h^{-1} Mpc. The virial mass is $2.1 \times 10^{14}\ h^{-1}\ M_\odot$. Correcting for faint cluster galaxies without redshifts and allowing for a modest evolution in the galaxy luminosity function gives a current epoch mass-to-light ratio $M/L_V(0) = 255\ h\ M_\odot/L_\odot$, comparable to Coma's 275 h. The same field contains galaxy groups at $z = 0.225$ and $z = 0.412$. The clusters' gravitational fields induce image ellipticities that are calculated from the light-traces-mass density distribution and compared with the tangential distortions observed by Fahlman et al. (1994). Between 1 and 3 virial radii, the observed lensing distortions are $\langle e_T \rangle = 0.054 \pm 0.017$, as compared to the $\langle e_T \rangle = 0.022 \pm 0.006$ that the light-traces-mass model and the virial M/L predict, hence the gravitational mass of the cluster appears to be at least 2.5 ± 1.1 times the virial mass.

Subject headings: galaxies: clusters: individual (MS 1224+20) — galaxies: distances and redshifts — galaxies: fundamental parameters — gravitational lensing

1. INTRODUCTION

The possibility that the total mass of galaxy clusters may be far larger than the virial masses calculated from their galaxy distributions has long been recognized, but is an observationally difficult problem. The virial mass statistic is not sensitive to mass beyond the mean harmonic radius of the (effectively massless) galaxies which trace the cluster potential. Cluster virial mass-to-light ratios (e.g., Kent & Gunn 1982) have relatively stable values, implying that $\Omega \simeq 0.2$, in close agreement with those inferred from the cosmic virial theorem (Bean et al. 1983; Davis & Peebles 1983). However, large-scale flow fields measure $\sigma_8 \Omega^{0.6}$ and generally are taken to imply that $\Omega \simeq 1$, with large confidence intervals and uncertainty as to the (sample-dependent) value of σ_8, the 8 h^{-1} Mpc sphere density contrast (e.g., Lynden-Bell, Lahav, & Burstein 1989; Bertschinger et al. 1990; Kaiser et al. 1991; Strauss et al. 1992; Nusser & Dekel 1993). The discrepancy between these measurements of Ω is somewhat surprising, since clusters of galaxies are the largest collapsed structures, and the comoving length scales R, from which they originate, are about 10 h^{-1} Mpc [$\sigma_v(1D) \simeq 1.1 H_0 R(1+z)^{1/2}$; e.g., White & Frenk 1991], which is only a factor of 3 smaller than the scales, 30 h^{-1} Mpc, on which the flows are measured.

Aside from the observational issue of establishing Ω, the determination of cluster masses is also a significant test of inflationary cosmology, which in its simplest form predicts $\Omega = 1$ (Guth 1981; Bardeen, Steinhardt, & Turner 1983). Some physical motivation for a galaxy-mass segregation of approximately the correct magnitude to allow cluster galaxies to greatly underestimate the true Ω-value is found within (some, not all) numerical simulations following the infall of galaxies into growing clusters (e.g., West & Richstone 1988; Carlberg & Dubinski 1991; Carlberg 1994). Observational evidence that virial masses underestimate total cluster masses or that light does not trace mass would be an important step in resolving these issues.

To measure galaxy cluster masses at radii well beyond the virial radius of course requires mass tracers at radii where the cluster density is rapidly declining (faster than r^{-2} according to simulation data). Galaxies themselves remain viable tracers, although the problem of unrelated field galaxies in the velocity space of the cluster becomes an important issue. X-ray flux diminishes as the square of the density, making the measurements difficult. The relatively new technique of weak gravitational lensing (e.g., Tyson, Valdes, & Wenk 1990; Miralda-Escudé 1991) has great promise as an indicator of the total mass.

In this paper we use a redshift survey of the MS 1224+20 cluster field to construct a light-traces-mass surface density map normalized using the mass-to-light ratio (M/L) from a virial analysis of the cluster. The weak gravitational lensing distortions are calculated from the mass map and compared with the distortions observed by Fahlman et al. (1994, hereafter FKSW). Our basic goal is to test whether the observed distortions are consistent with those predicted using the virial mass normalization. The next section discusses our observations, which we use in § 3 to derive the virial mass. In § 4 the surface brightness of the cluster is normalized with the virial M/L to predict the gravitational distortions, which we compare with the observed values.

2. OBSERVATIONS

The cluster MS 1224+20 (Gioia et al. 1990; Henry et al. 1992; Gioia & Luppino 1994) has a very high X-ray luminosity ($L_x \simeq 4.6 \times 10^{44}$ ergs s^{-1}) at $z = 0.325$ and is one of a uniform sample of moderate-redshift clusters for which we are doing a high-precision redshift survey. The cluster was observed at

[1] Guest Observer, Canada-France-Hawaii Telescope (CFHT), which is operated jointly by the Centre Nationale de la Recherche Scientifique of France, the National Research Council of Canada, and the University of Hawaii.

[2] Department of Astronomy, University of Toronto, 60 St. George Street, Toronto, Ontario, Canada M5S 1A1.

[3] Department of Astronomy, FM-20, University of Washington, Seattle, WA 98195.

[4] Center for Astrophysics and Space Astronomy, CB 389, University of Colorado, Boulder, CO 80309.

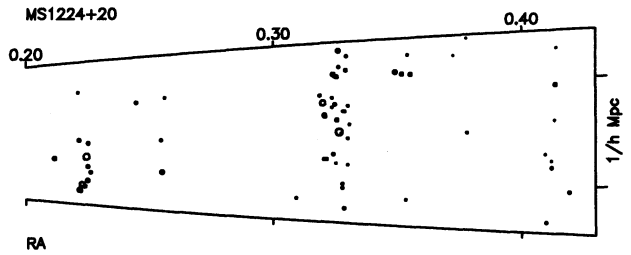

FIG. 1.—Redshifts plotted against the relative locations (in physical distance) in the right ascension direction with east at the top. There are eight more redshifts at $z > 0.42$.

CFHT during the nights UT 1993 January 24 and 25 using the Multiobject Spectrograph (MOS) as part of the Canadian Network for Observational Cosmology (CNOC) consortium redshift survey of galaxy clusters (see Carlberg et al. 1994). The cluster field (useful size 430″ × 540″, centered on the cD galaxy) was imaged in Gunn r and g filters for 900 s each. Using a variable point-spread function version of the faint galaxy photometry software system PPP (Yee 1991), two-color photometry and star-galaxy separation of all objects in the field was performed in real time. The resulting catalog was then used as input to a program which designed two complementary spectroscopic aperture masks for the MOS. For a detailed description of our observational techniques see Yee et al. (1994).

To obtain as many spectra per aperture mask as possible, a filter was used which limited the spectra to 4650–6100 Å. This range passes the [O II] emission feature at 3727 Å, the 4000 Å break region, and the G band (4304 Å) for objects in the $0.25 \lesssim z \lesssim 0.42$ range. This is optimal for identifying cluster members at $z = 0.32$, but introduces a strong redshift selection function for field galaxies. In particular, emission-line redshifts with $0.20 < z < 0.25$ are unlikely to be obtained, (as neither [O II] λ3727 nor [O III] $\lambda\lambda$4959, 5007 are observable), although we have identified a number of absorption-line galaxies with $z = 0.22$ in the field. Likewise, absorption-line galaxies with $z > 0.40$ are unlikely to be assigned redshifts. The nominal completeness limit for spectroscopy was set at $r = 21.5$ mag with a spectral resolution of 15 Å. Two masks, each with over 100 slits, were observed. The integration times were 2 × 2400 s for mask A and 2 × 3600 s for mask B, yielding a total of 75 redshifts in the field. There are 30 redshifts in the cluster, and a total of 47 are associated with the three largest structures in the field (see Figs. 1 and 2). The velocity uncertainty of each redshift is estimated by multiple observations of several galaxies and by simulations of galaxy spectra.

The observational procedures are designed to maximize the data rate, maintain a velocity accuracy of better than $\simeq 150$ km s^{-1}, and preserve the geometric distribution of the galaxies in the field (in particular the angular correlation function and the mean density of galaxies over the face of the cluster). A completeness function $C(m, x, y) = S(m)F(x, y)$, as a function of magnitude and position, is estimated by dividing the number of galaxies for which redshifts were obtained by the total number in that magnitude range. Owing to the sparseness of the data, the function is determined separately in magnitude and position. $S(m)$, derived using galaxies in the whole field, declines smoothly from 0.5 at $r = 20$ mag to 0.1 at $r = 22$ mag, where we truncate the sample. The entire $r = 17$–22 mag range is added together to determine the geometrical selection effects, $F(x, y)$. The variance of the selection function over the field is about 10%. All statistical quantities are geometrically weighted, which produces only a small correction to the unweighted data.

3. VIRIAL ANALYSIS

The MS 1224+20 field (Fig. 1) has a somewhat surprising amount of projected structure (given that X-ray selection reduces projection contamination), in particular a foreground cluster at $z = 0.22$ with a velocity dispersion of 500 km s^{-1} and a small cluster with a velocity dispersion of about 400 km s^{-1} at $z = 0.41$. The main cluster is taken to span the redshift range

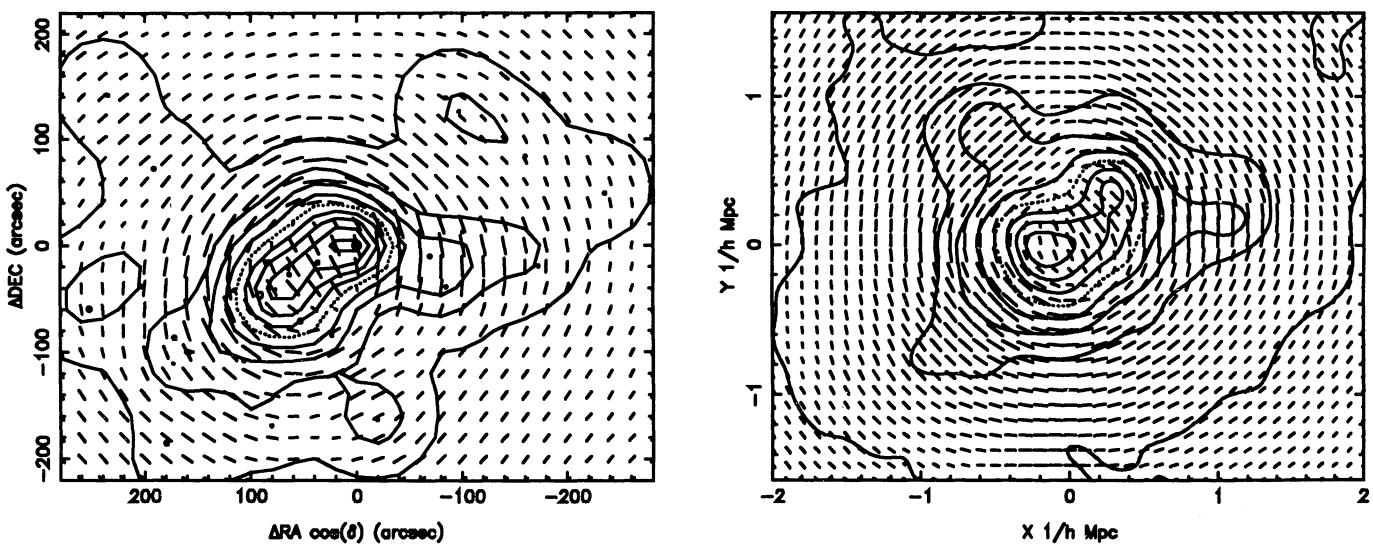

FIG. 2.—The "κ map" for the MS 1224+20 field (*left*) and a 1700 km s^{-1} cluster field drawn from a 10 × 10 × 100 h^{-1} Mpc region in an n-body simulation (*right*). The MS 1224+20 field is 1.6 h^{-1} Mpc in the right ascension direction. The contours on the left are smoothed with a 20″ Gaussian and plotted at 0.01 increments in κ. The "sticks" are proportional to the local image distortion.

from 0.318 to 0.331, with an average redshift of 0.3257. The velocity histogram has some internal structure (significant at the 95% level). This level of substructure is consistent with all other clusters in our survey, and is to be expected, since clusters are subject to constant gravitational infall.

The line-of-sight velocity dispersion of the cluster is $\sigma_v \simeq 770$ km s^{-1}, and the harmonic radius of the galaxies, r_h, is 112″, which is about half the field size in the smallest direction. The density of the cluster is falling rapidly beyond this radius, the slope of the surface brightness being $d \log \Sigma_L / d \log r = -1.5$. Consequently, the harmonic radius is not expected to be affected by the finite field size. The physical length subtended by the mean harmonic radius is 0.32 h^{-1} Mpc. The implied virial mass, $3\pi\sigma_v^2 r_h/2G$, is 2.1 × 10^{14} $M_\odot$. The rest-frame luminosity of the cluster to $r = 22$ mag is $L_V = 8.2 \times 10^{11}$ $L_\odot$, using $V - r = 0.17$ mag (Sebok 1986), and a K-correction of $K_V = -0.60$ mag (Coleman, Wu, & Weedman 1980). The color and K-correction are based on an average of elliptical galaxy and early-type spirals, as is appropriate for this cluster. The completeness correction for galaxies not observed spectroscopically has increased the luminosity 1.9 times over the observed galaxies. The rest-frame mass-to-light ratio M/L_V is equal to 250 h in solar units to this magnitude limit. To estimate the current epoch M/L, we approximate the luminosity evolution as $\Delta M \simeq z$. The light missed below our magnitude limit, 0.16 L_*, is calculated to be an additional 34%, assuming that the luminosity function can be represented as a Schechter function with $\alpha = 1.25$. The fully corrected $M/L_V(0) \simeq 255$ h, which is similar to the 275 h found for Coma (Kent & Gunn 1982). A bootstrap analysis (for the entire sample, not only the cluster galaxies) finds that the 1 σ error of $M/L_V(0)$ is 30%, with less than 0.1% probability that $M/L_V(0)$ exceeds 500 h.

The two other structures in the field, at redshifts 0.22 and 0.412, have, respectively, only 12 and seven spectroscopic redshifts, giving velocity dispersions of 500 and 400 km s^{-1}. Both have M/L values consistent with that obtained for the 0.33 cluster (but with substantial uncertainties).

4. THE LIGHT TRACES-MASS MAP AND WEAK LENSING

To test the assumption that the cluster light traces the mass in the cluster, and in particular whether the cluster light is more concentrated than the cluster mass, we use the observed galaxy distribution and the M/L ratio to estimate the surface density of the cluster. The 47 relevant redshifts will of course only be good for a fairly noisy image. These same galaxies are used in FKSW for comparison with their estimate of lensing surface density. Note that the resulting mass map does not depend on the photometric K-corrections. The surface density map, smoothed with a 20″ Gaussian filter, is displayed in the left-hand panel of Figure 2. The contours are linear in mass density. For comparison, a cluster of velocity dispersion $\simeq$1700 km s^{-1} drawn from a 128^3 particle, 100 h^{-1} Mpc box n-body simulation (CDM with $\sigma_8 = 1$) is displayed on the right-hand side of Figure 2.

The predicted image distortions (in the weak-field limit) under the assumption that the light traces the mass are the "sticks" in Figure 2. The distortions are calculated using the two-dimensional Poisson equation, $\nabla^2\phi = -2\kappa$, summed over the three structures at different redshifts, where $\kappa = \Sigma/\Sigma_c(z_l, z_s)$. The inverse critical surface density, in angular coordinates, for a structure at redshift z, is $(\Sigma_c^\theta)^{-1} = 4\pi G c^{-2}(1 + z_l) r_l^{-1}(1 - r_l/r_s)$, where the subscripts l and s denote the lens and the source redshift. For $\Omega = 1$ the comoving coordinate distances are $r(z) = 2cH_0^{-1}[1 - (1 + z)^{-1/2}]$. The total image distortion is $(\gamma_1^2 + \gamma_2^2)^{1/2}$ (where, $\gamma_1 = \frac{1}{2}(\phi_{xx} - \phi_{yy})$, $\gamma_2 = \phi_{xy}$ (e.g., Schneider, Ehlers, & Falco 1992).

The tangential ellipticity is defined as $e_T = \gamma_1 \cos 2\theta + \gamma_2 \sin 2\theta$, where θ is the polar coordinate angle about the chosen center. For a circularly symmetric mass distribution $e_T = \bar{\Sigma}(<r) - \Sigma(r)$ in critical units, where $\bar{\Sigma}$ is the mean interior mass density, $M(<r)/\pi r^2$. The right-hand panel of Figure 3 shows this quantity (*stars*) for a region 10 × 10 × 100 h^{-1} Mpc surrounding the n-body cluster smoothed with a 0.1 h^{-1} Mpc Gaussian filter, and normalized to the same critical density as MS 1224+20. At all radii the annular averages of $\langle e_T \rangle$ and $\bar{\Sigma}(<r) - \Sigma(r)$ are nearly equal. At large radii $\langle e_T \rangle$ converges to $\bar{\Sigma}$, and $\langle e_T \rangle$ is a useful statistic to compare whether a given mass distribution is compatible with observed lensing. In the center the structural details make $\langle e_T \rangle$ a poor estimator of $\bar{\Sigma}$.

To compute the expected lensing distortions, the sources are taken to be at $z_s = 0.6$, in common with FKWS. This is an important assumption (for which there is strong supporting evidence), since a given measured shear implies larger masses for lower redshift sources. The redshifts of cluster and background imply a critical surface density of 7.5 × 10^{15} $M_\odot$ h^2 Mpc^{-2}. The expected lensing distortions are tiny. At a projected distance of 0.5 h^{-1} Mpc from the cluster, i.e., about 1.5 virial radii, the virial mass implies a mean interior density of

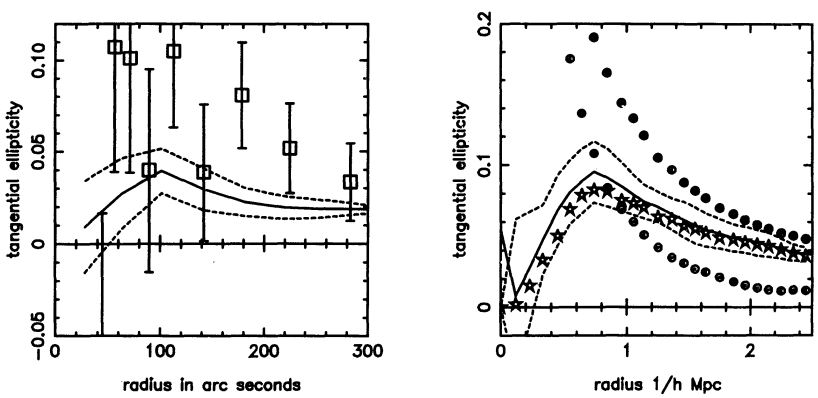

FIG. 3.—Gravitational lensing image distortions for MS 1224+20 (*left*) and the n-body cluster of Fig. 2 (*right*). The solid line gives the predicted $\langle e_T \rangle$, and dashed lines show the variance around the annulus. Both plots use the inferred center of mass (same as that of FKSW for MS 1224+20). On the right, $\bar{\Sigma} - \Sigma$ (*stars*), $\bar{\Sigma}$ (*circled plus signs*), and Σ (*circled dots*) are shown, demonstrating the usefulness of $\langle e_T \rangle = \bar{\Sigma} - \Sigma$ and that at large radii $\langle e_T \rangle$ converges to the mean interior density.

0.03 in critical units, which somewhat overestimates the expected $\langle e_T \rangle$.

To compute $\langle e_T \rangle$ in an annulus, a center must be chosen. We use the same center as FKSW, about 70″ east and 20″ south of the cD. This location is close to the center of symmetry of the light. Figure 3 displays the averaged tangential ellipticities predicted from the light distribution (*solid line*) and the observed values (*squares*). The variance in the annulus of the predicted $\langle e_T \rangle$ is shown as dashed lines; the observed values have error flags that give the error of the mean. The main result is that the observed lensing is considerably stronger than predicted by the virial M/L ratio.

Between 100″ and 300″ the average observed tangential image distortion, $\langle e_T \rangle = 0.054 \pm 0.017$, is significantly greater than the predicted value, 0.022. The predicted value would be about 30% lower if the $z = 0.33$ cluster alone were used in the prediction. A comparison with the n-body data shown in the right-hand panel of Figure 3 gives confidence that this measurement is not very sensitive to asymmetries. Based on $\langle e_T \rangle$, the surface density of MS 1224+20 is 2.5 ± 1.1 times the value that the light-traces-mass model gives in the 100″–300″ range, where the 30% uncertainty in the virial normalization is included in quadrature.

5. DISCUSSION AND CONCLUSIONS

Combining a dynamical analysis of visible galaxies and the weak distortion map of background galaxies allows a powerful test of the hypothesis that cluster mass distributions are more extended than their light distribution. The MS 1224+20 cluster turns out to be a relatively difficult case, since it is not particularly rich in galaxies, its relatively low velocity dispersion does not give very strong image distortions, and the two other projected structures in the field complicate the analysis. The cluster has a velocity dispersion of 770 km s^{-1} and a virial radius of 0.32 h^{-1} Mpc. The virial radius is somewhat smaller than a comparable $z = 0$ cluster, but within our field the cluster becomes "clumpy" and has a steep (logarithmic slope $> -3/2$) density profile beyond this radius. The M/L ratio, K-corrected and allowing a luminosity evolution of 0.3 mag, is 255 h, with a 1 σ error of 30%, entirely compatible with Coma's 275 h value, which in conjunction with a field luminosity density is taken to imply that $\Omega \simeq 0.2$. The average tangential ellipticity observed by FKSW is about 2.5 times larger than the values predicted by the light-traces-mass model (for sources at an average $z_s = 0.6$).

What would it take to bring the virial mass and the lensing mass into agreement? Doubling the cluster $M/L_V(0)$ to about 500 h would remove the discrepancy, but this M/L is less than 0.1% probable based on a bootstrap error analysis. The cluster may not be dynamically well relaxed; the cD is displaced by about half the virial radius from the region of greatest galaxy density to the southeast, and the galaxies to the west have somewhat higher redshifts. However, the cD's velocity is an insignificant 150 km s^{-1} greater than the cluster mean velocity. Clusters that are out of dynamical equilibrium normally have virial masses higher than their true mass, which would increase the discrepancy between the "relaxed" virial mass and the lensing mass. These clusters with strong X-ray emission all have fairly red galaxy populations, making the K-corrections fairly well determined. Therefore, the difference is not likely to be found in the virial analysis, which gives a perfectly normal $M/L_V(0)$. The mass inferred from lensing depends on the background galaxies being distributed with the redshifts extrapolated from field surveys and the increase in numbers with depth. If the sources were at $z_s = 3$, then the inferred mass is halved from the $z_s = 0.6$ assumed here; however, such a high redshift seems quite unlikely in samples limited at $I = 22$ and 23 based on current redshift information. Calculating angular size distances with a low Ω or assuming a very clumpy universe gives about a 10% cluster-mass reduction. The analysis certainly could be refined if the source galaxies had individually known redshifts. The redshift diagram, Figure 1, illustrates that the redshift distribution is extremely clumpy in a field this small, suggesting that the background galaxies may be similarly distributed. Nevertheless, the observed distortions, about 0.06 at nearly 0.7 h^{-1} Mpc, are far too large to be a result of the virial mass alone, which predicts about 0.02 at this radius.

We thank Greg Fahlman, Nick Kaiser, Gordon Squires, and David Woods for the use of their data. The observations reported here are a small subset of the CNOC cluster mapping project, whose members we thank for assistance and use of these data. Chris Pritchet, Roberto Abraham, and Tammy Smecker-Hane were an invaluable part of the observing team.

REFERENCES

Bardeen, J. M., Steinhardt, P. J., & Turner, M. S. 1983, Phys. Rev. D, 28, 679
Bean, A. J., Efstathiou, G., Ellis, R. S. Peterson, B. A., & Shanks, T. 1983, MNRAS, 205, 605
Bertschinger, E., Dekel, A., Faber, S. M., Dressler, A., & Burstein, D. 1990, ApJ, 364, 370
Carlberg, R. G. 1994, ApJ, 433, 468
Carlberg, R. G., & Dubinski, J. 1991, ApJ, 369, 13
Carlberg, R. G., et al. 1994, JRASC, 88, 39
Coleman, G. D., Wu, C. C., & Weedman, D. W. 1980, ApJS, 285, 426
Davis, M., & Peebles, P. J. E. 1983, ApJ, 267, 465
Fahlman, G., Kaiser, N., Squires, G., & Woods, D. 1994, ApJ, in press (FKSW)
Gioia, I. M., & Luppino, G. A. 1994, ApJS, 94, 583
Gioia, I. M., Maccacaro, T., Schild, R. E., Wolter, A., Stocke, J. T., Morris, S. L., & Henry, J. P. 1990, ApJS, 72, 567
Guth, A. 1981, Phys. Rev. D, 23, 347
Henry, J. P., Gioia, I. M., Maccacaro, T., Morris, S. L., Stocke, J. T., & Wolter, A. 1992, ApJ, 386, 408
Kaiser, N., Efstathiou, G., Ellis, R., Frenk, C., Lawrence, A., Rowan-Robinson, M., & Saunders, W. 1991, MNRAS, 252, 1
Kent, S., & Gunn, J. E. 1982, AJ, 87, 945
Lynden-Bell, D., Lahav, O., & Burstein, D. 1989, MNRAS, 241, 235
Miralda-Escudé, J. 1991, ApJ, 370, 1
Nusser, A., & Dekel, A. 1993, ApJ, 405, 437
Schneider, P., Ehlers, J., & Falco, E. E. 1992, Gravitational Lenses (New York: Springer-Verlag)
Sebok, W. L. 1986, ApJS, 62, 301
Strauss, M. A., Yahil, A., Davis, M., Huchra, J. P., & Fisher, K. 1992, ApJ, 397, 395
Tyson, J. A., Valdes, F., & Wenk, R. A. 1990, ApJ, 349, L1
West, M. J., & Richstone, D. O. 1988, ApJ, 335, 532
White, S. D. M., & Frenk, C. S. 1991, ApJ, 379, 52
Yee, H. K. C. 1991, PASP, 103, 396
Yee, H. K. C., Ellingson, E., Carlberg, R. G., & Pritchet, C. J. 1994, in preparation